New diamond nanofabrication process for hard x-ray zone plates

Fredrik Uhlén,[a] Sandra Lindqvist, Daniel Nilsson, Julia Reinspach, Ulrich Vogt, Hans M. Hertz, and Anders Holmberg
Biomedical and X-Ray Physics, Department of Applied Physics, Royal Institute of Technology, 106 91 Stockholm, Sweden

Ray Barrett
ESRF, F-38043 Grenoble Cedex 9, France

(Received 28 June 2011; accepted 1 October 2011; published 28 October 2011)

The authors report on a new tungsten-hardmask-based diamond dry-etch process for fabricating diamond zone plate lenses with a high aspect ratio. The tungsten hardmask is structured by electron-beam lithography, together with Cl_2/O_2 and SF_6/O_2 reactive ion etching in a trilayer resist-chromium-tungsten stack. The underlying diamond is then etched in an O_2 plasma. The authors demonstrate excellent-quality diamond gratings with half-pitch down to 80 nm and a height of 2.6 μm, as well as zone plates with a 75 μm diameter and 100 nm outermost zone width. The diffraction efficiency of the zone plates is measured to 14.5% at an 8 keV x-ray energy, and the imaging properties were investigated in a scanning microscope arrangement showing sub-100-nm resolution. The imaging and thermal properties of these lenses make them suitable for use with high-brightness x-ray free-electron laser sources. © *2011 American Vacuum Society*. [DOI: 10.1116/1.3656055]

I. INTRODUCTION

During recent years it has become important to develop zone plates that can be used with the new and upcoming x-ray free-electron laser sources[1,2] that operate in the 2–12 keV photon energy range. In addition to the usual challenges with producing x-ray zone plates, i.e., sub-100-nm high-aspect-ratio periodic patterning, these zone plates need to withstand the high heatload that such high-brightness sources will impose upon the optics.[3,4] Traditionally, high-Z materials, e.g., Ta,[5] Au,[6] Ir,[7] and W[8] have been used for 2 to 12 keV zone plates, but the high heat load can deteriorate the metal or even melt it. Diamond (Di) is considered the optimal zone plate material for such applications due to its high thermal conductivity (2052 W/mK at 300 K) and good optical properties for hard x-rays, i.e., low absorbtion.[4]

Zone plates focus x-rays by diffraction and can be considered as a circular diffraction grating with radially decreasing linewidth.[9] For focusing and imaging applications, there are two primary properties of the zone plate to consider. Firstly, the resolution is directly proportional to the outermost zone width. Thus a narrow width is desirable, and typical zone widths for fabricated hard x-ray zone plates are in the range of 25 to 100 nm.[5–8] Secondly, the diffraction efficiency is defined as the fraction of incident light diffracted into a certain diffraction order of the zone plate. Normally, the first order diffraction is considered. The efficiency is primarily determined by the optical material and its thickness[9] but will be decreased due to fabrication errors, e.g., deviation from a 1:1 line-to-space ratio and aspect-ratio dependent etch rate. Figure 1 shows the theoretical diffraction efficiency at 12.4 keV for W, Au, and Di as a function of thickness. As can be seen, the thickness needed for the maximum efficiency requires a very high aspect ratio for narrow zones. In the fabrication, a trade-off must be made between the desired smallest zone width and the highest aspect ratio that can be fabricated. For example, for state-of-the-art hard x-ray Au zone plates, the outermost zone width is 25 nm with a height of 300 nm.[6] Zone plates made from Di have also recently been demonstrated with a width of 100 nm and a thickness of 2.2 μm.[10]

The nanostructuring of Di is primarily achieved via O_2-plasma-based etching. To reach high aspect ratios, different combinations of hardmasks and O_2 recipes have been used. For the Di zone plate,[10] a 500 nm thick hydrogen silsequioxane (HSQ) mask was used with pure O_2 etching. In other published work related to the construction of highly anisotropic Di structures, Ni-Ti[11] and Al[12] have been used as hardmasks.

In the present paper we describe a new nanofabrication process that uses W as a hardmask for making high aspect-ratio CVD Di structures. We present Di gratings with half-pitch down to 80 nm and a height of 2.6 μm. We also show zone plates with 100 nm outermost zones and present the results from diffraction efficiency and imaging experiments conducted at the European Synchrotron Radiation Facility (ESRF) in Grenoble.

II. NANOFABRICATION

Figure 2 shows the nanofabrication process. Electron-beam lithography is used to pattern the zone plate into an e-beam resist. The pattern is then transferred into the Di via three subsequent reactive-ion-etching steps, in which W is used as a hardmask for etching Di. The process steps are described in detail below.

First, the stack of material is prepared. A 400 nm thick layer of W is deposited onto a (5×5) mm^2, 100 μm thick CVD Di substrate (Diamond Materials GmbH) via dc magnetron sputtering (AJA Orion system, 10^{-8} mbar base pressure). The sputtering is done at the following parameters: 20 SCCM Ar gas flow, 5 SCCM N_2 gas flow, 3 mTorr pressure,

[a]Electronic mail: fredrik.uhlen@biox.kth.se

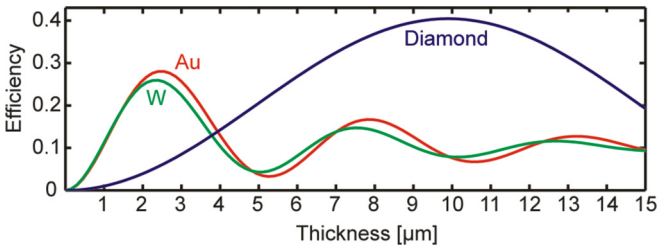

FIG. 1. (Color online) Theoretical diffraction efficiency as a function of zone height for the materials W, Au, and Di at 12.4 keV.

75 W power, and 250 °C sample temperature, for a deposition time of 100 min (SCCM denotes cubic centimeters per minute at standard temperature and pressure). Using these parameters yields a low-stress film with little surface roughness. Then, a 20 nm thick layer of Cr is electron-beam evaporated (Edwards Auto 306 System, 10^{-6} mbar base pressure) onto the W. Finally, an 80 nm thick positive e-beam resist (Zep 7000, Zeon Chemicals L.P.) is spin-coated on top of the stack and subsequently baked in an oven at 170 °C for 30 min. Electron-beam lithography (Raith 150 system) is used to pattern the e-beam resist. The exposure is done at 25 kV with a typical dose of 100 μC/cm^2. The pattern is then developed by immersing the sample into hexylacetate for 30 s and then rinsing it in isopropanol and pentane for 15 s and 5 s, respectively. The e-beam pattern is transferred to the Cr layer via reactive ion etching (RIE) (Oxford Instruments, Plasmalab 100 system) in a Cl_2/O_2 plasma at the following parameters: 8 SCCM Cl_2 gas flow, 2 SCCM O_2 gas flow, 20 mTorr pressure, 10 W rf power, 10 W inductively coupled plasma (ICP) power, 20 °C sample temperature, and an etch time of 4 min 45 s. The Cr is then used as a hardmask for etching W with a SF_6/O_2 RIE process. An anisotropic etch in W is important, and good balance between volatile products and sidewall passivation is required. The SF_6 plasma contains radicals that react with W and produce volatile products.[13] O_2 combined with a low temperature produces a nonvolatile film on sidewalls, accounting for sidewall passivation.[14] The recipe used in our RIE system has been optimized with respect to temperature and rf power in order to achieve an anisotropic etch. The recipe parameters are 8 SCCM SF_6 gas flow, 2 SCCM O_2 gas flow, 10 mTorr pressure, 40 W rf power, and a sample temperature of −20 °C. This results in an etch rate of approximately 35 nm/min and an etch time of ∼12 min. Some overetching is required in order to clear the W in narrow trenches. A final O_2 RIE step (Oxford Instruments, Plasmalab 80+ system) to etch the Di with W as a hardmask is performed at the following parameters: 10 SCCM O_2 gas flow, 3 mTorr pressure, 100 W rf power, 200 W ICP, and 20 °C sample temperature. The etch rate is 30 nm/min, and thus an etch time of 1 to 3 h is required in order to etch 2 to 5 μm into the Di. Any remaining Cr from the W etch is sputtered away in the O_2 etch within the first 10 min.

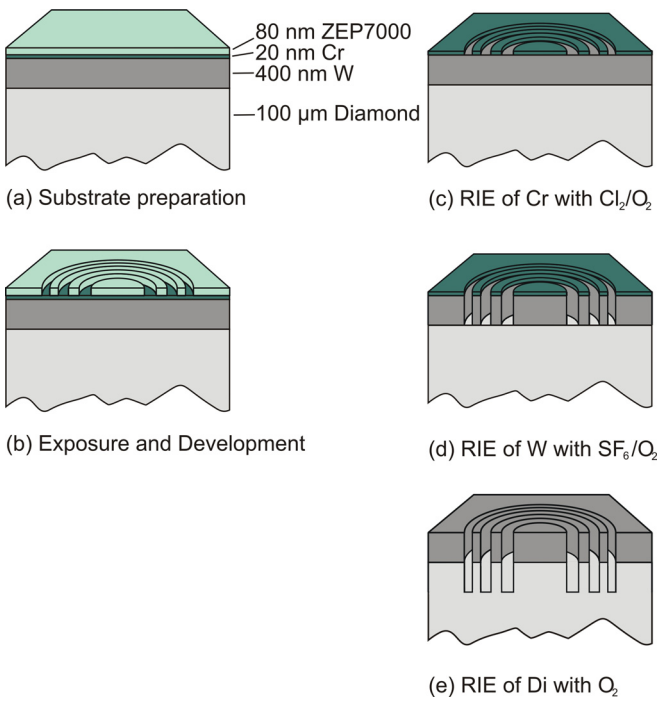

FIG. 2. (Color online) Fabrication process for diamond zone plates. After substrate preparation (a), the zone plate pattern is first written in the e-beam resist via electron beam lithography and then developed (b). Subsequently, the pattern is transferred to the Cr layer via RIE with Cl_2/O_2 (c). It is then etched into the W via RIE with SF_6/O_2 (d). Finally, an O_2 RIE step is employed to transfer the pattern into the diamond (e).

Figure 3 displays the anisotropic etch profile of W for 100 and 60 nm half-pitch gratings. The structures are 570 nm high, which yields aspect ratios of 1:6 and 1:10, respectively. Presently, the smallest half-pitch that can be fabricated in W is ∼50 nm. This limit is primarily set by the proximity effect in the lithography step, in which incoming electrons are backscattered by the high-Z W, exposing unwanted areas. However, using other resist processes might improve the resolution and make smaller line widths possible.[15,16]

Figure 4 shows the result of etching Di using W as a hardmask for half-pitches of 100 nm, 80 nm, and 60 nm. When etching the Di, the smallest linewidth that can be transferred successfully from the W pattern is 80 nm. We believe that the main difficulty in etching smaller half-pitches is that W is redeposited on the sidewalls, resulting in the prevention of etching in the narrow trenches. For 100 and 80 nm half-pitch, the gratings are of high quality and yield aspect ratios

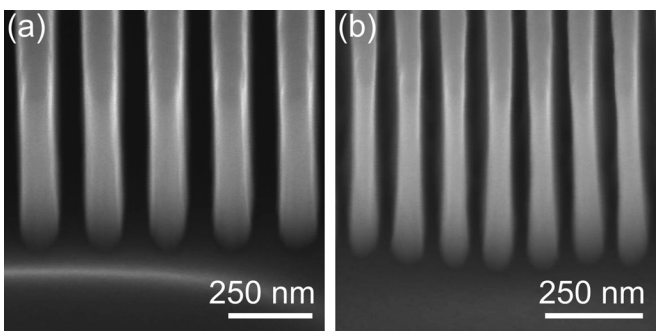

FIG. 3. W gratings with (a) 100 nm and (b) 60 nm half-pitch etched at a sample temperature of −20 °C. Tilt angle is 52°.

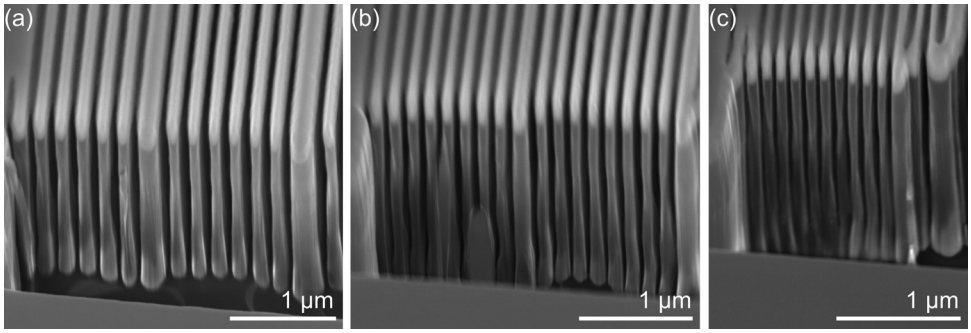

FIG. 4. Diamond gratings with half-pitches of 100, 80, and 60 nm. The diamond height is 2.6 μm. The pattern transfer for lines with half-pitches down to 80 nm is good. For the 60 nm lines, W redeposition into the trenches decreases the etch rate. The white layer is the remaining W. Tilt angles are 35°, 40°, and 40°, respectively.

of 26:1 and 32:1, respectively, for a Di grating structure 2.6 μm in height. To our knowledge, these are the highest reported aspect ratios in diamond in these small dimensions. As can be seen in Fig. 4 and Fig. 6, a thin white layer (approximately 100 to 200 nm) of W from the hardmask is still present.

Figure 5 shows a Di zone plate fabricated with the new process. The diameter is 75 μm and the outermost zone width is 100 nm, resulting in a focal length of 75 mm at 12.4 keV. In Fig. 6, a focused-ion-beam cross-sectional cut of the zone plates has been performed in order to show the zone profile. In the outermost parts with a 100 nm zone width, the etch profile is good and the Di height is 2 μm. The O_2 recipe results in an aspect-ratio-dependent etch rate, resulting in an etch depth of 4.5 μm in the inner parts and 2 μm at the outer zones.

III. ZONE PLATE CHARACTERIZATION

In order to characterize the fabricated zone plates, diffraction efficiency measurements and 2D imaging were performed at the ID06 beamline at ESRF in Grenoble. The x-ray beam energy during the experiments was 8 keV, and the higher undulator harmonics were suppressed by detuning the monochromator. For these experiments, a zone plate with an outermost zone width of 100 nm, an average Di etch depth of 2.2 μm, and a 250 nm remaining W layer was used.

Figure 7(a) shows the experimental arrangement for the diffraction efficiency measurement. A 100 μm diameter aperture is placed upstream of the zone plate. Behind the zone plate, a 10 μm pinhole is positioned in the first-order focus in order to record the intensity from this order only. The intensity is measured with an x-ray diode. After a reference intensity measurement (without a Di window), the ratio of the first-order focus intensity and the reference intensity gives the total diffraction efficiency. In this experiment we

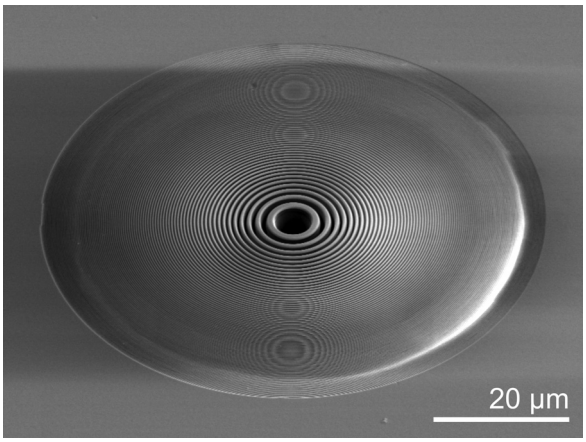

FIG. 5. Fabricated diamond zone plate. The diameter is 75 μm, and the outermost zone width is 100 nm, resulting in a focal length of 75 mm at E = 12.4 keV. Tilt angle is 45°.

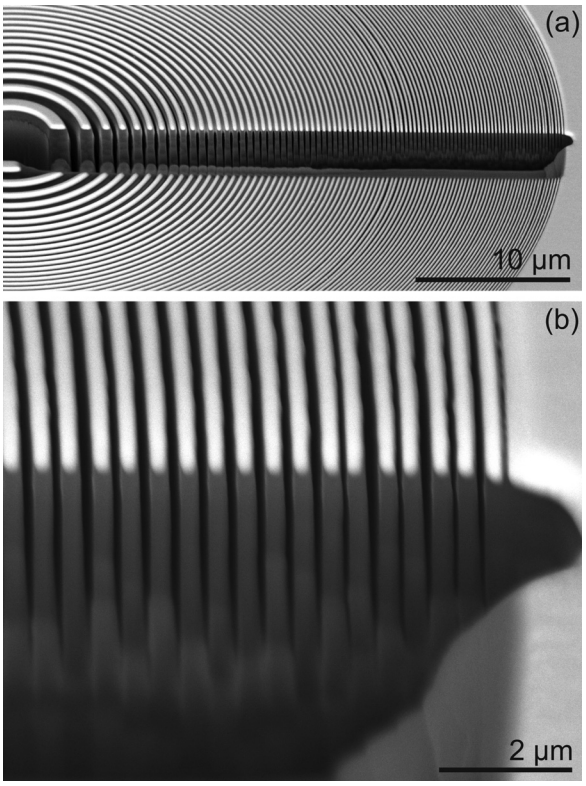

FIG. 6. Zone plate with a focused-ion-beam cross-sectional cut along its radius. The white layer is the remaining W. (a) The whole cut from center to periphery. (b) The outermost zones. The outermost zone width is 100 nm, and the etch depth in the outer part is 2.1 μm. Tilt angle is 52°.

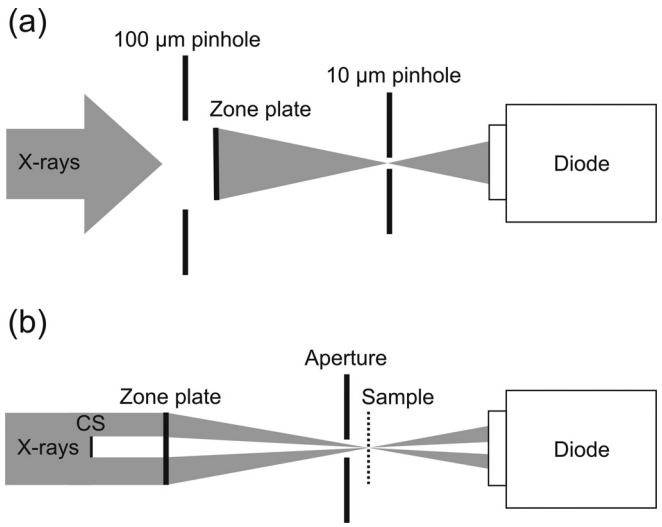

FIG. 7. (a) Experimental arrangement for the total diffraction efficiency measurement. (b) Experimental arrangement for imaging. CS = central stop.

measured an average efficiency of 14.5%, which corresponds to 80% of the theoretical value at 8 keV. It should be mentioned that in this case, in which a relatively thick hardmask remains, the W contributes to about one-third of the efficiency. Furthermore, the remaining 98 μm thick diamond absorbs about 14% of the radiation. If necessary, i.e., if the zone plate will be used under a very high heatload, any remaining W layer could be removed by a SF_6/O_2 plasma.

The imaging properties of the zone plate were investigated using an x-ray scanning microscope arrangement, Fig. 7(b). A central stop is placed in front of the zone plate in order to minimize the zeroth order contribution from the beam. An aperture is then positioned a short distance in front of the focus to include only the first diffraction order. Finally, an Au zone plate is placed in the focus as a test sample. The Au zone plate has a 100 nm outermost zone width and a thickness of 700 nm. A piezo-driven stage provides accurate sample translation. The image is reconstructed by recording the intensity at each point and scanning the sample in a raster-fashion. Figure 8 shows a 2D scan of the outermost part of the Au zone plate, where the 100 nm lines and spaces are clearly resolved. The modulation in the image is around 0.04, whereas the contrast in the sample is approximately 0.14. As a first estimation, this would yield a total modulation of 0.28.

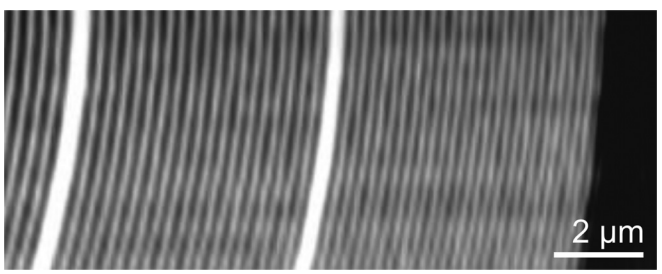

FIG. 8. 2D image of an Au zone plate with a 100 nm outermost zone width. All zones are clearly resolved, showing the diamond zone plate's capability of 100 nm resolution imaging.

IV. SUMMARY AND OUTLOOK

In this paper we have presented a new fabrication process for Di zone plates. A W hardmask with 60 nm half-pitch grating lines and an aspect ratio of ~10:1 has been shown. The dry etch into the Di resulted in down to 80 nm half-pitch and 2.6 μm high gratings, which corresponds to an aspect ratio of 32:1. The limiting factors in achieving narrower pitches are the electron-beam lithography resolution and the redeposition of the W hardmask in the narrow trenches. The diffraction efficiency of a fabricated Di zone plate with a 100 nm outermost zone was measured to 14.5% at a photon energy of 8 keV. An imaging resolution of 100 nm was demonstrated in a 2D scanning microscope arrangement.

In the future we will implement new resist processes to improve the pattern quality and further decrease the smallest achievable pitch. The Di O_2 etch parameters will also be optimized in order to minimize the sputtering effect of the hardmask during the etching.

ACKNOWLEDGMENTS

The authors gratefully acknowledge the financial support of the Swedish Science Research Council, the Swedish Foundation for Strategic Research, the Wallenberg Foundation, and the European Community's Seventh Framework Programme (FP7/2007-2013) under Grant No. 226716. Thanks to C. David of the Paul Scherrer Institute (CH) for providing the central stop used for resolution tests.

[1]LCLS Conceptual Design Report, Stanford, 2002, ssrl.slac.stanford.edu/lcls/cdr/; European XFEL Technical Design Report, Hamburg, 2007, xfel.desy.de/tdr/tdr/; and SCSS Conceptual Design Report, Japan, 2005, www-xfel.spring8.or.jp/.
[2]H. N. Chapman *et al.*, Nat. Phys. **2**, 839 (2006).
[3]R. A. London *et al.*, in *Optics for Fourth-Generation X-Ray Sources*, edited by R. Tatchyn, K. F. Andreas, and T. Matsushita, *Computational simulations of high-intensity x-ray matter interaction* (SPIE, San Diego, CA, 2001), pp. 51–62.
[4]D. Nilsson, A. Holmberg, H. Sinn, and U. Vogt, Nucl. Instrum. Methods Phys. Res. A **621**, 620 (2010).
[5]A. Osawa, T. Tamamura, T. Ishii, H. Yoshihara, and T. Kagoshima, Microelectron. Eng. **35**, 525 (1997).
[6]Y. Feng, M. Feser, A. Lyon, S. Rishton, X. Zeng, S. Chen, S. Sassolini, and W. Yun, J. Vac. Sci. Technol. B **25**, 2004 (2007).
[7]J. Vila-Comamala, S. Gorelick, E. Färm, C. M. Kewish, A. Diaz, R. Barrett, V. A. Guzenko, M. Ritala, and C. David, Opt. Express **19**, 175 (2010).
[8]P. Charalambous, in *X-Ray Microscopy: Proceedings of the Sixth International Conference*, Berkeley, CA, 2–6 August 1999, *Fabrication and characterization of tungsten zone plates for multi KeV X-rays*, edited by T. Warwick, W. Meyer-Ilse, and D. Attwood (American Institute of Physics, Melville, NY, 2007).
[9]D. Attwod, *Soft X-Rays and Extreme Ultraviolet Radiation* (Cambridge University Press, New York, 1999), p. 340.
[10]C. David *et al.*, Scientific Reports **1** (2001).
[11]G. F. Ding, H. P. Mao, Y. L. Cai, Y. H. Zhang, X. Yao, and X. L. Zhao, Diamond Relat. Mater. **14**, 1543 (2005).
[12]H. Shiomi, J. Appl. Phys. **36**, 7745 (1997).
[13]A. Picard and G. Turban, Plasma Chem. Plasma Process. **5**, 333 (1985).
[14]A. L. Goodyear, S. Mackenzie, D. L. Olynick, and E. H. Anderson, J. Vac. Sci. Technol. B **18**, 3471 (2000).
[15]J. Reinspach, F. Uhlén, H. M. Hertz, and A. Holmberg, "A 12-nm half-pitch W-Cr-HSQ trilayer process for soft x-ray tungsten zone plates," J. Vac. Sci. Technol. B **29**, 06FG02–1 (2011).
[16]J. Reinspach, M. Lindblom, O. von Hofsten, M. Bertilson, H. M. Hertz, and A. Holmberg, J. Vac. Sci. Technol. B **27**, 2593 (2009).